

---

This is an electronic reprint of the original article.  
This reprint may differ from the original in pagination and typographic detail.

Kämpjärvi, Petteri; Sourander, Mauri; Komulainen, Tiina; Nikus, Mats; Vatanski, Nikolai;  
Jämsä-Jounela, Sirkka-Liisa

## **Fault detection and isolation of an online analyzer for an ethylene cracking process**

*Published in:*  
Control Engineering Practice

Published: 01/01/2008

*Document Version*  
Peer-reviewed accepted author manuscript, also known as Final accepted manuscript or Post-print

*Please cite the original version:*  
Kämpjärvi, P., Sourander, M., Komulainen, T., Nikus, M., Vatanski, N., & Jämsä-Jounela, S.-L. (2008). Fault detection and isolation of an online analyzer for an ethylene cracking process. *Control Engineering Practice*, 16, 1-13.

# Fault detection and isolation of an on-line analyzer for an ethylene cracking process

Petteri Kämpjärvi<sup>a</sup>, Mauri Sourander<sup>b</sup>, Tiina Komulainen<sup>c</sup>, Nikolai Vatanski<sup>c</sup>, Mats Nikus<sup>c</sup>, Sirkka-Liisa Jämsä-Jounela<sup>c</sup>

<sup>a</sup> Neste Oil Oy, Porvoo refinery, P.O. Box 310, FIN-06101 Porvoo, Finland

<sup>b</sup> Neste Jacobs Oy, Process and Automation Technology, P.O. Box 310, FIN-06101 Porvoo, Finland

<sup>c</sup> Laboratory of Process Control and Automation, Helsinki University of Technology, P.O. Box 6100, FIN-02150 HUT, Finland

## Abstract

Fault diagnosis methods based on process history data have been studied widely in recent years, and several successful industrial applications have been reported. Improved data validation has resulted in more stable processes and better quality of the products. In this paper, an on-line fault detection and isolation system consisting of a combination of principal component analysis (PCA) and two neural networks (NNs), radial basis function network (RBFN) and self-organizing map (SOM), is presented. The system detects and isolates faulty operation of the analyzers in an ethylene cracking furnace. The test results with real-time process data are presented and discussed. ©2007 Elsevier Ltd. All rights reserved

## Keywords

Ethylene cracking, Process monitoring, Fault detection, Fault isolation, Principal component analysis, Self-organizing map

## 1 Introduction

On-line process monitoring with fault detection can provide stability and efficiency for a wide range of processes. Early detection and isolation of abnormal and undesired process states and equipment failures are essential requirements for safe and reliable processes. Process analysis based on statistical or neural network (NN) methods promotes understanding of the process phenomena, and ultimately improves plant performance. In recent years, there has been increasing interest among researchers in applying different process monitoring and fault diagnosis methods. A large number of applications have been reviewed, e.g. by Isermann and Ballé (1997) and Patton, Uppal, and Lopez-Toribio (2000). Both reviews indicate that there is a growing tendency to augment quantitative model-based methods with NNs and fuzzy logic.

Venkatasubramanian, Rengaswamy, Kavuri, and Yin (2003) and Venkatasubramanian, Rengaswamy, Yin, and Kavuri (2003) published a review of monitoring methods, especially those applied in the field of chemical processes. They classified the methods according to the form of process knowledge used. One category is based on process models, and includes both qualitative causal models and quantitative methods. The other category is based on process history, and includes both qualitative (e.g. rule based) and quantitative methods (NNs and multivariate statistical methods).

Common features of the statistical methods used are their ability to reduce correlations between variables, compress data, and reduce the dimensionality of the data. These characteristics enable efficient extraction of the relevant information and analysis of the data. The most important statistical monitoring methods are based on principal component analysis (PCA) and partial least-squares regression (PLS). Dynamic variants of PCA and PLS consider the dynamic nature of the monitored process and analyze both cross-correlation and auto-correlation of the variables. The dynamic methods are especially suitable for continuous processes with long time delays and varying throughputs on process variables (Chen, McAvoy, & Piovoso, 1998; Ku,

Storer, & Georgakis, 1995). Recursive methods for PCA and PLS have been proposed by Li, Yue, Valle-Cervantes, and Qin (2000) and Qin (1998). The recursive methods are especially suitable for time-dependent processes with slow changes. Multi-scale principal component analysis (MSPCA), a combination of PCA and wavelet analysis, removes the autocorrelations of variables by means of wavelet analysis, and eliminates cross-correlations between variables with PCA (Misra, Yue, Qin, & Ling, 2002). The method is suitable for processes with auto-correlated measurements and time-varying characteristics. Nonlinear principal component analysis (NLPCA) is a combination of NNs and PCA. Dong and McAvoy (1996) proposed an NLPCA method, which integrates a principal curve algorithm and NNs. The idea of this method is to fit curves instead of lines to the data with the help of a feedforward network.

NN architectures can be divided into three categories: feedforward, feedback and self-organizing networks. According to Kohonen (1990), NNs are the most applicable to classification and regression problems, which do not need perfect precision. The availability of large amounts of data is especially important. The self-organizing map (SOM), introduced by Kohonen, is an unsupervised NN that has been compared to NLPCA, because it adapts to the structure of the data. The weights of the neurons are changed in the training process so that the neurons are fitted to the densest regions of the data. A neural net based on adaptive resonance theory (ART) differs fundamentally from a SOM in the fact that the size and shape of the map are not determined beforehand. The ART map has many modifications, including combinations of ART maps, like ART3 and ARTnet, and hybrids of ART maps and fuzzy logic in fuzzy ARTMAP (Wienke et al., 1996; Rallo, Ferre-Gine, Arenas, & Giralt, 2002). Radial basis function networks (RBFNs), introduced by Broomhead and Lowe (1988) and Moody and Darken (1989), fit input data to radial basis functions, whereas traditional feed forward networks usually compare input signals to data vectors. RBFN is suitable for fault diagnosis. Wavenets are combination of wavelets and NNs with hierarchical multiresolution learning (Bakshi & Stephanopoulos, 1993). This type of NN is especially suitable for low dimension, dynamic fault diagnostic problems (Zhao, Chen, & Shen, 1998).

Most of the articles in the field focus on the use of only one fault isolation method. Although all the statistical methods are based on process history data, each method examines the problem in a slightly different way. Comparative studies have been made between process history-based methods, e.g. by Bergman, Sourander, and Jämsä-Jounela (2002), Jämsä-Jounela, Vermasvouri, Enden, and Haavisto (2003) and Chiang, Russel, and Braatz (2000).

Although several process fault detection and isolation methods have been proposed in recent years, little research is being carried out on how to identify the right variables for these methods and how to capture the essence of process knowledge. Many chemical processes exhibit strong nonlinearity and, unfortunately, there are only a few measurements that directly relate to the fundamental process variables characteristic to the process. Therefore, the direct use of the available process measurements often poorly describes the process behavior, and the fundamental process variables or their approximations have to be derived from the measurements by calculations. This obviously improves the identification capabilities of most monitoring methods, as demonstrated in the previous studies of a similar nature by Jämsä-Jounela, Laine, and Ruokonen (1998), Yoon and MacGregor (2001), Bergman et al. (2002), and Komulainen, Sourander, and Jämsä-Jounela (2004). A fundamental understanding of the relationships between process variables is essential in creating the right computed process variables. On the other hand, the use of irrelevant and often noisy measurements usually deteriorates the monitoring performance.

Model predictive control (MPC) has been widely applied in the chemical industries. Good measurement accuracy and consistency are prerequisites for good control, and errors in controlled variables especially can cause the process to enter undesirable operating regimes. Data validation is needed for better MPC performance. Pranatyasto and Qin (2001) applied PCA to detect and identify sensor faults under MPC control, and reported that its performance with data validation was superior to that without.

In this paper, an on-line fault detection and isolation system that monitors the measurements of an ethylene cracking process is presented. The faults studied comprise different types of dynamic disturbance, malfunctions, degradations of the process, and its instrumentation such that they, at least temporarily, produce incompatible analyzer and process measurement signals while the process is still in an acceptable production state. The main task was to determine the instances when the content measurements of on-line analyzers cannot be relied on for automatic control purposes. Erroneous measurements are detected and the external feedback is temporary suspended in the studied control application until validated measurements are again available. This paper first describes the ethylene cracking process, then outlines the application, and finally presents and discusses the results from industrial implementations and performance testing periods.

## 2 Description of the ethylene cracking process and its control strategy

### 2.1 Process description

Ethylene cracking, which involves endothermic pyrolysis reactions, is carried out in large, gas-fired furnaces containing parallel tubular reactor coils. The furnaces consist of three major sections: the convection section, the cracking reactor in the radiant box, and the transfer line exchange (TLE) section. The cracking furnace in this study has four parallel passes. The schematic diagram of a classical ethylene cracking furnace is shown in Fig. 1. The feed and effluent compositions are analyzed by taking conditioned samples containing C<sub>4</sub> compounds and lighter hydrocarbons (HC). Thus, the heavier compounds and hydrogen for instance in the feed and effluent are not measured. In the effluent, the sum of measured compounds varies around 70 mol% of the conditioned sample. The cracking of hydrocarbons within the temperature range 800–850 °C produces a mixture of hydrogen, methane, ethylene, propylene, butenes, butadiene, aromatics, acetylenes, etc. The hydrocarbon feedstock and its diluent steam are preheated in the convection section to 600–650 °C and then fed to the radiant section where the main cracking reactions occur. The effluent is cooled in a few milliseconds in the TLE in order to stop the secondary reactions. Notable reactions occur when the temperature is over 700 °C.

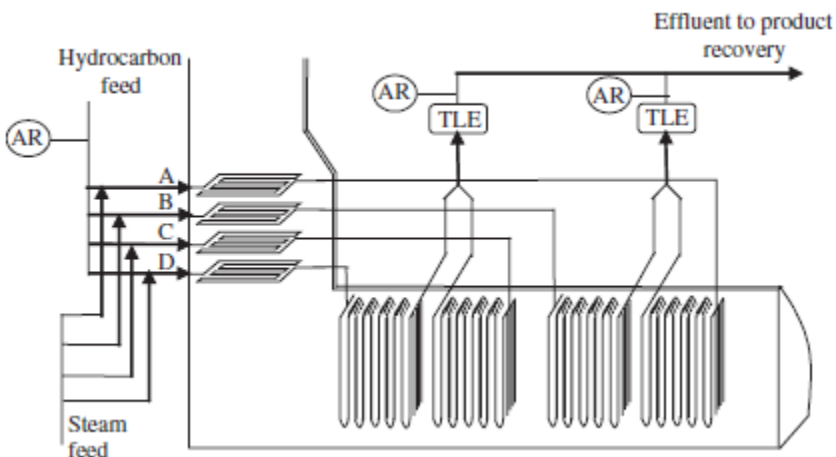


**Fig. 1.** Schematic diagram of an ethylene cracking furnace. In the diagram, each circle with the letters AR represents a gas chromatograph analyzer

The operating regime, permitted by the furnace process design, is exceptionally large. Several feedstocks are used and they can be in either liquid or gas phase. The normal variation in the feedstock composition of this furnace ranges from all possible mixtures of ethane, propane and butane, while the other feed constituents are essentially impurities. The process conditions are adjusted on the basis of the feedstock composition. As the feedstock composition changes dynamically, the other process variables have to follow

the change, but usually with relationships that are nonlinear over the large operating window. The effluent temperature, for instance, can vary between 800 and 840 °C. The largest differences, however, occur in the effluent component content. The methane content normally varies between 5 and 35 mol%, the lower range being typical for feed mixtures consisting mainly of ethane and the higher range for mixtures consisting mainly of propane and butanes. For a constant feed composition, the normal methane variation from other sources can be from 1 to 5 mol%. The ethylene content normally varies between 25 and 36 mol% for the same reasons as for methane, and the normal variation for a given feed composition varies from 3 to 6 mol%. The variation of ethane, propane and propylene is presented in [Table 1](#).

**Table 1**

Input variable set of the study

Variable	Description	Unit	Min	Max
1	Feed ethane content	mol%	8.9	89.8
2	Feed propane content	mol%	1.8	79.2
3	Effluent ethane content	mol%	5.4	22.1
4	Effluent propane content	mol%	0.3	9.8
5	Effluent propylene content	mol%	1.8	11.2
6	Effluent methane to propylene ratio	mol/mol	2.8	8.3
7	Effluent ethylene content	mol%	25.3	33.5
8	Coil effluent temperature	deg K	1071	1115
9	Effluent ethane to feed ethane ratio	mol/mol	0.32	3.5
10	Effluent propane to feed propane ratio	mol/mol	0.09	0.24
11	Effluent ethylene to feed ethane ratio	mol/mol	0.41	3.04
12	Effluent propylene to feed propane ratio	mol/mol	0.12	0.63
13	Effluent propane to ethane ratio	mol/mol	0.01	1.85
14	Sum of feed components/sum of effluent components	mol/mol	1.12	1.61
15	Effluent ethylene content to effluent temperature ratio	mol%/deg K	0.02	0.03
16	Effluent temperature to feed ethane content ratio	deg K/mol%	12.5	122
17	Effluent temperature to feed propane content ratio	deg K/mol%	14.0	590
18	HC feed rate to feed ethane content ratio	T/h/mol%	0.11	1.0
19	HC feed rate to feed propane content ratio	T/h/mol%	0.11	4.9
20	Steam rate to feed ethane content ratio	T/h/mol%	0.04	0.5
21	Steam rate to feed propane content ratio	T/h/mol%	0.04	2.4
22	Effluent ethane content to HC feed rate ratio	mol%/t/h	0.58	2.5
23	Sum of effluent components	mol%	62	82
24	Sum of feed components	mol%	90	99
25	Kinetic model methane to propylene ratio parameter	–	0.97	1.09

## 2.2 Process control description

The furnace is controlled by a model predictive controller (MPC) that includes severity and conversion control. For conversion control the key measurement values are provided by the on-line analyzers, which analyze the hydrocarbon composition of the feed and of the effluent. The sampling times of the analyzers are between 15 and 20 min, and the dead time between sampling from the effluent line and completion of the analysis is around 7 min. Nonisothermal differential equation process models, based on hydrocarbon decomposition kinetics and process measurements for the tubular reactor, are used to predict the effluent composition between sampling intervals. These predictions are also used as feedback in the MPC. Kinetic parameters of these conversion and effluent composition prediction models are adjusted online by the MPC application to match the validated analysis results of the on-line analyzers. As the analyzers are part of the closed loop, it is very important that only correctly analyzed and validated estimates for compositions are used for model parameter adjustment.

The reactor conversion MPC application also features temperature, feed rate, and steam rate pass balancing, total feed rate control and constraint control. Coil outlet temperatures, fuel pressures, hydrocarbon feed and steam feed rates are manipulated variables for the MPC.

### 3 Methods for handling process nonlinearities in industrial FDI systems

In order to construct a successful fault detection and isolation (FDI) system, the nonlinearity of the process has to be handled in the design and construction of the system. To achieve this, two approaches could be used, as demonstrated in the application part of this paper. In the first approach, a linear method that is enhanced by adding nonlinearity to the input set data is used. In the second approach, the nonlinear method is applied directly.

#### 3.1 PCA augmented with the nonlinear computed variables in the input set

A common method used in FDI systems is the well-known PCA method. This method has, however, some inherent problems due to its linear structure. Several efforts have been made to handle nonlinearities within the PCA framework. The first reported approach was generalized PCA (GPCA) by Gnanadesikan (1977). In this method, the original data set is expanded with the cross products and powers of the original variables. As an example, if one wants to include quadratic nonlinear dependency among variables  $x_1$  and  $x_2$  then the input data vector can be augmented by the three variables  $x_1^2$ ,  $x_2^2$  and  $x_1x_2$ :

$$x' = [x_1 \ x_2 \ x_1^2 \ x_2^2 \ x_1x_2]. \quad (1)$$

The author also expanded the method to incorporate general, but known nonlinearities:

$$X' = [x_1 \ x_2 \ \dots \ x_m \ f_1(x_1, x_2, \dots) \times \dots \ f_n(x_1, x_2, \dots)] \quad (2)$$

where  $x_i$  are the measurement vectors  $l \times 1$ ,  $l$  is the number of observations. This method permits the number of necessary principal components (PC) needed to describe the data to be reduced, but it also generates excessive information. Jolliffe (2002) proposed that the calculated variables in GPCA should replace the original variables instead of being added to the data set, thus reducing the dimensionality of the problem:

$$X^* = [f_1(x_1, x_2, \dots) \ f_2(x_1, x_2, \dots) \ \dots \ f_n(x_1, x_2, \dots)]. \quad (3)$$

A natural application of GPCA is to use process knowledge when determining the functions for the added variables. Such process knowledge can be, e.g. a computed variable determined by multiplying the volumetric flow rate by the corresponding temperature that describes the energy flow into the system. For unknown nonlinearities, truncated power series expansions can be used as an approximation. In some cases this addition of computed variables will convert the data set into a more linear form, thus improving the performance of the PCA. Mathematically linear equations are present in the PCA model as zero magnitude eigenvalues, and the final model can then be based on fewer principal components.

The main benefit of the approach is that the method is based on the well-known PCA method, the use of which is well established in practice. The number of adjusted parameters is relatively low, thus making it applicable in real industrial environments. The process knowledge can be easily added by any experienced plant engineer.

The main drawback of the approach is that determination of the proper computed variables may be an iterative procedure, with some heuristics involved.

### *3.2 Direct modeling of the fault state using the nonlinear methods*

PCA methods only model the normal operating conditions and provide information about faulty situations. Fault isolation can be performed to some extent using contribution plots, but their reliability may be inadequate. Direct nonlinear methods can be used as a complementary or alternative approach for handling the process nonlinearities and improving isolability. Such models directly describe the dependence between observed process conditions and the corresponding fault case. To perform this task, methods such as, e.g. multi-layer perceptrons (MLP), RBFN or SOM can be used.

In this paper a combined PCA/RBFN/SOM-system, improved with process knowledge, was used for handling the nonlinearities and performing fault isolation.

## **4 Description of the FDI system**

An on-line fault detection and isolation system was developed for enhancing the analyzer fault detection in an ethylene cracking process (Kämpjärvi, 2002). The main aim of the FDI system was to determine when the composition measurements provided by the on-line analyzers cannot be relied on for MPC use. The goal was to detect analyzer faults, validate the feed and effluent analyzer results, and to produce validation signals to be used by the MPC application online. The detected faults are classified as feed analyzer, effluent analyzer or other fault types using two independent neural nets in parallel.

Examination of the past process data showed that most of the known disturbances occurring in the process are related to the analyzed process streams, which underlines the importance of focusing on analyzer validation in lieu of the other process and instrument faults.

### *4.1 Structure and implementation of the FDI system*

The FDI system developed for analyzer monitoring consists of a combination of three different methods: PCA, a SOM, and a RBFN. The PCA was used to detect the abnormal situations and to provide information about the state of the process, and the NNs, SOM and RBFN, were used to isolate the faults and classify them as either feed analyzer or effluent analyzer faults. The main outputs of the proposed system were divided into three different classes: normal state of the analyzers, a fault in the feed analyzer and a fault in the effluent analyzer. As a supplementary output, the system provides information about the process state.

The input of the FDI system consists of two data sets,  $\mathbf{X}'$  and  $\mathbf{X}''$ , which include the process measurements augmented with two computed variable sets according to Eq.(2). The PCA model was trained with the set  $\mathbf{X}'$ , the RBFN with input set  $\mathbf{X}''$ , and the SOM with the PCA residuals  $E$ . The output of the system is the square prediction error (SPE) index from the PCA model, and two complementary outputs from the NNs that provide information about the analyzer fault type. The outputs are further evaluated in the decision logic block, where the final decisions about the analyzer state, as well as the process state, are given. An analyzer fault is declared only if the outputs of both NNs are in agreement. Otherwise, a nonanalyzer fault is declared. The structure of the FDI system is illustrated in Fig. 2. The structure is novel in the sense that this type of three-method system has not been reported before in petrochemical industry applications.

The FDI system was implemented in the Windows NT environment using MATLAB 6.0 and its toolboxes. Neural net toolbox was used to implement the RFB networks, and SOM Toolpak, which is a function package developed by the Laboratory of Computer and Information Science (CIS), Helsinki University of

Technology, was used to implement the SOMs. The ODBC link available at the ethylene cracker real-time process database was used to interface with the FDI system in the local network.

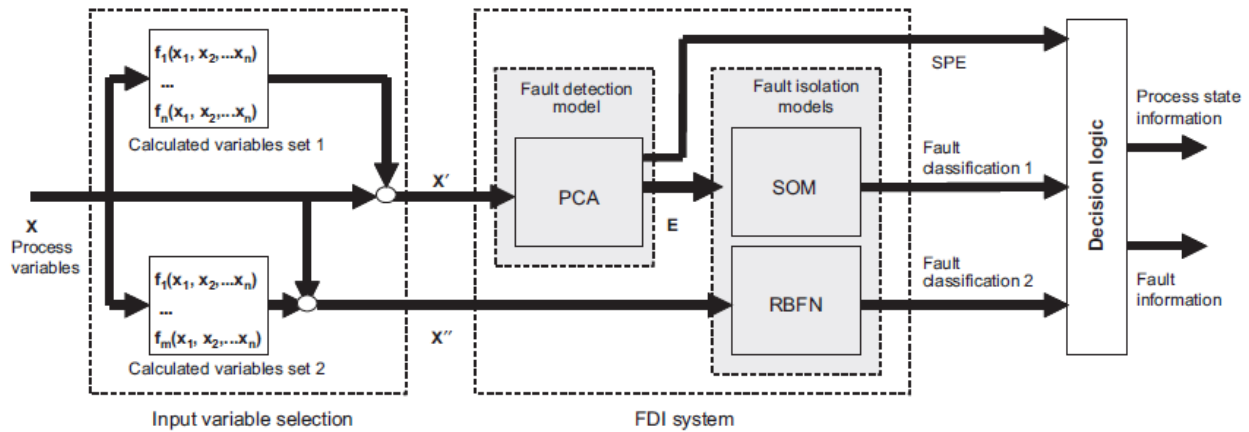


**Fig. 2.** Schematic diagram of the FDI system for the analyzers in the ethylene cracking process

#### 4.2 Selection of the input variables for the FDI system

Proper process variable selection is a critical factor for a successful FDI system application. Both direct and computed variables were included in the FDI system input variable set.

The computed variables were mainly based on the simplified equations of the nonlinear kinetic models that are used in the MPC application to predict the effluent composition. The conversion of individual components present in the feed and reactor effluent was simplified by calculating ratios between effluent and corresponding feed composition variables. The relationship between the pyrolysis reaction temperature and conversion was approximated using ratios involving temperature and effluent composition. The modeling ability of the computed variables was verified using a nonlinear dynamic process simulator of the ethylene cracking furnace for both normal operating conditions and analyzer fault cases.

The input variable set, presented in Table 1, was used throughout the study. The most relevant hydrocarbon contents in the feedstock of the furnace were ethane (variable 1) and propane (variable 2). All the effluent analyzer measurements (variables 3–7) and the coil outlet temperature (variable 8) were used as inputs. The other variables (variables 9–25) included in the model were computed process variables that provided an insight into the nonlinear process characteristics.

Computed variables 9–21 all indicate faults when the conversion rates change inconsistently with the other variables. Computed variables 9–14 are necessary in order to distinguish the cases where the conversion rate is changing inconsistently due to sensor failure and those due to real disturbance. The aim of computed variables 15–17 is to add an indication of temperature measurement failure, and of computed variables 18–21 an indication of faults in the hydrocarbon and feed rate measurements. The other computed variables provide an indication of other disturbances.

##### 4.2.1 Conversion-related computed variables

Computed variables 9–14, which are related to changes in the conversion, together with inconsistent changes in the other process variables, indicate analyzer faults. The effluent ethane to feed ethane ratio (variable 9) reacts to changes in ethane conversion and changes in the feedstock ethane content through the amount of unreacted ethane. The effluent propane to feed propane ratio (variable 10) is similarly related to propane conversion. The effluent ethylene to feed ethane ratio (variable 11) reacts to changes in ethane to



ethylene conversion and changes in the feedstock composition. The feed ethylene (impurity) is summed with the feed ethane content, because the ethylene reactions in the furnace are slow. The effluent propylene to feed propane ratio (variable 12) describes the propane to propylene conversion rate. The feed propylene (impurity) was added to the feed propane. The effluent propane to effluent ethane ratio (variable 13) describes the unreacted portion of the feed components in the effluent, and it follows the changes in feed composition. The variable provides information about the discrepancy between the feed composition and corresponding effluent compositions. The sum of feed components to sum of effluent components ratio (variable 14) describes the influence of the unmeasured feed and effluent components, e.g. hydrogen in the feed, and hydrogen, butene and acetylene in the effluent.

#### 4.2.2 Temperature-related computed variables

Changes in ratios 15–17, together with inconsistent changes in other conversion-related variables, indicate an error in the corresponding compound analyzer or temperature measurement. The effluent ethylene to effluent temperature ratio (variable 15) describes the nonlinear effect of temperature on the conversion of all feed components. In contrast to the effluent ethylene content (variable 7), this ratio changes in a more linear fashion. The effluent temperature to feed ethane ratio (variable 16) describes the difference between the ethane-rich gas case and propane- and butane-rich gas cases. Ethane-rich gas is cracked at higher temperatures than a feedstock rich in other components. The effluent temperature to feed propane ratio (variable 17) describes the difference between the propane-rich gas case and the ethane- and the butane-rich gas cases. Propane-rich gas is cracked at different temperatures than feedstock rich in other components.

#### 4.2.3 Hydrocarbon and feed rate related computed variables

Changes in ratios 18–21, together with inconsistent changes in other process variables, indicate an error in the corresponding compound analyzer and hydrocarbon or feed rate measurement. The feed rate to feed ethane content ratio (variable 18), HC feed rate to feed ethane and feed propane content ratio (variable 19), steam rate to feed ethane content ratio (20) and steam rate to feed propane content ratio (variable 21) decrease the sensitivity of the fault detection to the measurement noise in the HC feed and steam rate. Furnaces can be charged at different rates, which introduces substantial variation in the feed rate and steam rate measurements.

#### 4.2.4 Other computed variables

The effluent ethane to HC feed rate ratio (variable 22) describes the conversion rate in ethane-rich feedstock cases. In ethane-rich feedstock cases, feed rate changes cannot usually be compensated by the appropriate temperature change, and this leads to a conversion rate change. A change in the conversion rate is reflected as variation in the effluent ethane content. The sum of effluent components (variable 23) describes the amount of analyzed effluent components lighter than C<sub>4</sub>. This variable describes the amount of unmeasured by-products, thus providing information about other reactions. Similarly, the sum of feed components (variable 24) contains information on other species entering the coil. The kinetic model effluent methane to propylene ratio parameter (variable 25) characterizes changes in the feedstock and process. It is adjusted online by the MPC application in order to match the kinetic process model with the process measurements. This variable is used to independently check the functioning of the analyzer.

### 4.3 Model training and variable selection of the PCA, SOM and RBFN models

#### 4.3.1 Training the PCA model

The 25 variables, presented in Table 1, were used as inputs ( $\mathbf{X}'$ ) for the PCA. The data covariance was formed according to

$$\mathbf{C} = \frac{1}{N-1} (\mathbf{X}')^T \mathbf{X}'. \quad (4)$$

Next the eigenvalue–eigenvector decomposition was performed:

$$C = V\Lambda V^T, \quad (5)$$

where  $V$  contains the eigenvectors and  $\Lambda$  contains the eigenvalues on the diagonal.

A number  $m$  of eigenvectors describing a large part of the data variation is included in the model:

$$X' = TV_m^T + E = \sum_{i=1}^m t_i p_i^T + E = \hat{X}' + E, \quad (6)$$

where

$$T = X'V_m \quad (7)$$

and  $V_m$  contains the first  $m$  eigenvectors.

The process data used in training represented normal operation conditions. The process operation for the period with normal data collected for PCA was checked by plant experts in order to ensure that it conformed to normal process and analyzer functioning.

About 15 successive days of 1-min data from the process were collected and analyzed (approximately 21,500 measurement points). The training set was constructed to include approximately equal number of hours of data from different process conditions by removing the excess steady state repeats (hours with no new information). The resulting data set (about 8000 measurements) contained 7400 sets of normal data, as asserted by plant experts, and these were used to train the PCA model. The rest of the data contains process disturbances and sensor failures.

A model with five principal components was selected for the FDI system. The model explains 95% of the variance in the 25 input variables of the original data, as shown in Fig. 3.

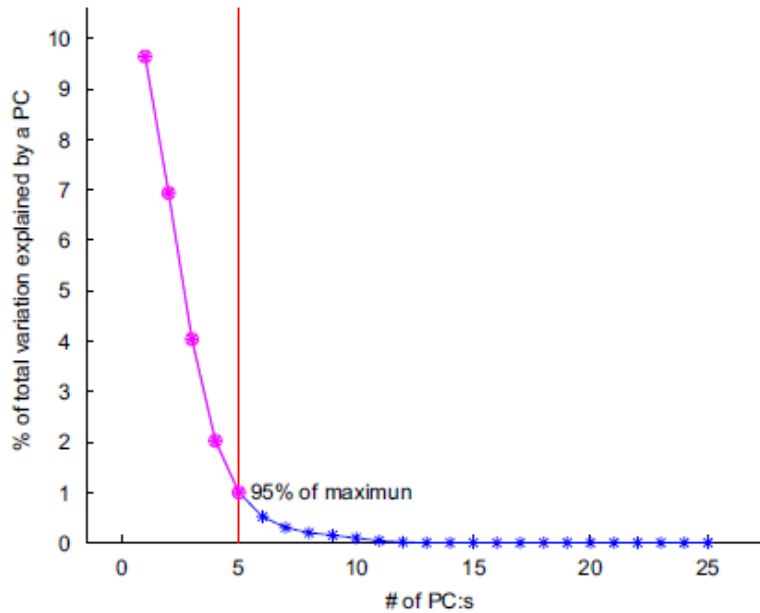


**Fig. 3.** PCA model selected for the FDI system

For the first two principal components, the most important variables were those related to the ethane and propane contents (variables 1–4). In the third PC, the other outlet compositions (variables 5–7), ethylene included, had a considerable effect. Also the sums of the compositions in the outlet and inlet (variables 23–24) had a considerable effect on the third PC. One of the most significant variables for the fourth principal component was the coil outlet temperature (variable 8). The methane/propane kinetic model parameter (variable 25) was the most influential variable in the fifth PC.

#### 4.3.2 Training the NN models

The data used for training the networks were selected from the ethylene plant process history data to represent both normal data and sets of single analyzer faults (one at a time). Because the number of faults was relatively low and the durations short, the repeat number of normal data had to be further reduced, while still retaining the essential richness of the variation of the original data.

The SOM was trained with 1200 data points, and the data set contained the faults necessary to model the faulty conditions. The residuals ( $\mathbf{E}$ ) to the PCA model, calculated according to Eq. (8), were used as inputs to the SOM:

$$\mathbf{E} = \mathbf{X}'(1 - \mathbf{V}_m \mathbf{V}_m^T). \quad (8)$$

The basic training procedure of SOM is defined as follows. First the winning node or best matching unit (BMU) is selected by finding the node that minimizes the Euclidian norm between this node and the data-point presented to the network at time instant  $k$ :

$$\{i, j\} = \arg \min_{ij} \|e(k) w_{ij}^{SOM}(k)\|. \quad (9)$$

Next the weights are updated according to the global network updating phase from iteration  $k$  to iteration  $k+1$  as

$$w_{ij}^{SOM}(k+1) = \begin{cases} w_{ij}^{SOM}(k) + \alpha(k)[e(k) - w_{ij}^{SOM}(k)], & \text{if } (i, j) \in N_c(k), \\ w_{ij}^{SOM}(k) & \text{if } (i, j) \notin N_c(k), \end{cases} \times \quad (10)$$

where the  $w_{ij}^{SOM}$ 's represent the weight vectors of the SOM nodes,  $\alpha$  is a learning rate parameter that decreases as the training progresses and  $N_c$  is a neighborhood around the winning node. After the first training step, learning vector quantification (LVQ) was used to further improve the separation between fault classes.

The trained SOM map is shown in Fig. 4. The normal states are indicated with blue, faults in a feed analyzer with pink, and faults in an effluent analyzer with red. The size of the colored circles indicates how many times each map unit was the BMU for the data set. As can be seen, the normal and fault states are separated relatively distinctly.

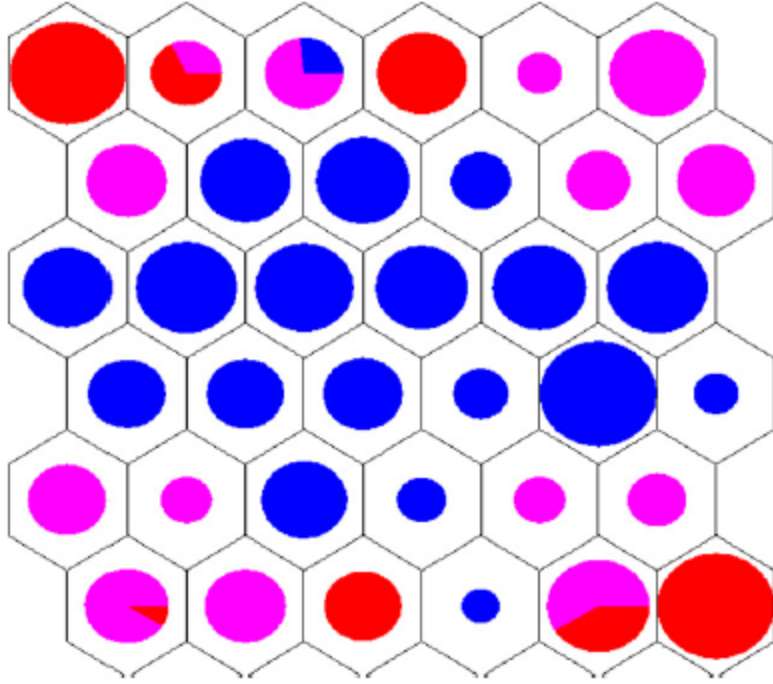


**Fig. 4.** The trained SOM map. Normal states are indicated with blue, faults in a feed analyzer with pink, and faults in an effluent analyzer with red

An alternative model for isolating the faults was developed based on the RBFN structure and was trained on a subset  $\mathbf{X}''$  of  $\mathbf{X}'$ , i.e. variables 1–6, 8–15. The variables excluded from the inputs were determined on the basis of a performance study using different input-sets to the RBFN.

The basis function used was the Gaussian function

$$g_j(x) = \exp\left(-\frac{1}{\gamma} \|\mathbf{x}'' - \mathbf{v}_j\|^2\right), \quad (11)$$

where  $\gamma$  is the spread of the radial basis function.

The output of the network is calculated as

$$F_j(\mathbf{x}'') = \sum_{i=1}^N w_{ji}^{RBF} g_i(\mathbf{x}'') \quad j \in \{1, 2\}, \quad (12)$$

where  $j$  describes fault types 1 and 2.

The RBF network was trained with 1700 data points using a two-step clustering and least-squares procedure. The network consisted of  $N=35$  basis functions (Eq. (11)). The width ( $\gamma$ ) of the radial basis function was set to 15. The desired outputs of the training data and the outputs of the RBF network are shown in Fig. 5. The faults in a feed analyzer are shown in the left window, and the faults in an effluent analyzer in the right window.

As can be seen from Fig. 5, the RBF network distinguishes very well between different faults and normal states in the training data.

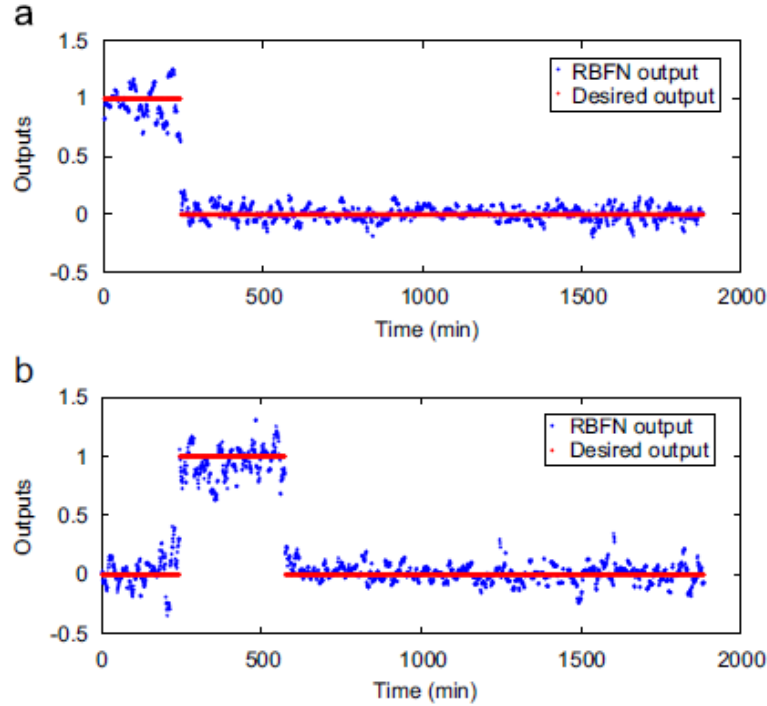


**Fig. 5.** (a) The desired outputs of the training data and the outputs of the RBF network, feed analyzer case  
(b) The desired outputs of the training data and the outputs of the RBF network, effluent analyzer case

## 5 The monitoring results and discussions

### 5.1. Monitoring results

After the FDI system had been trained, its fault detection and isolation abilities were evaluated using the process data that had not been used in training the system. During the 6-week test period, there were some analyzer and sample system problems that lead to measurement errors. Other disturbances also occurred during the test period in the process.

The FDI system diagnoses data once a minute and classifies it into three different classes. The normal state is marked with zero, a fault in the feed analyzer with 1, and a fault in the effluent analyzer with 2. An additional output of the system is the information about the state in the process provided by the SPE value of the PCA.

Summarizing the FDI system gave 61 alarms during the testing period. The proportion of incorrectly detected faults was very small, only 0.2%. The diagnosis system classified the detected fault states into two classes at 80% accuracy.

Next, some typical cases like feed and effluent analyzer faults, as well as process disturbances caused by variations in the fuel gas, are discussed and a summary of the results is presented.

#### 5.1.1. Case 1: measurement error of the effluent analyzer

The performance of the FDI system during a measurement error of the effluent analyzer is first discussed. The fault detection results of the diagnosis system are presented for a portion of the test data in Fig. 6a. The graph shows that the FDI system detects the occurrence of a measurement error (at time 1120) that lasts for half an hour. It is also clear from the PCA output (values of SPE violating the threshold) that an abnormal

situation has occurred in the process. The measurement error of the analyzer causes the SPE value to increase, as is illustrated in Fig. 6b. The rise is a consequence of the asynchronous sampling times of the analyzers. This refers to the fact that the analyzer measurements do not exactly match the temperatures at the sampling times of the analyzer.

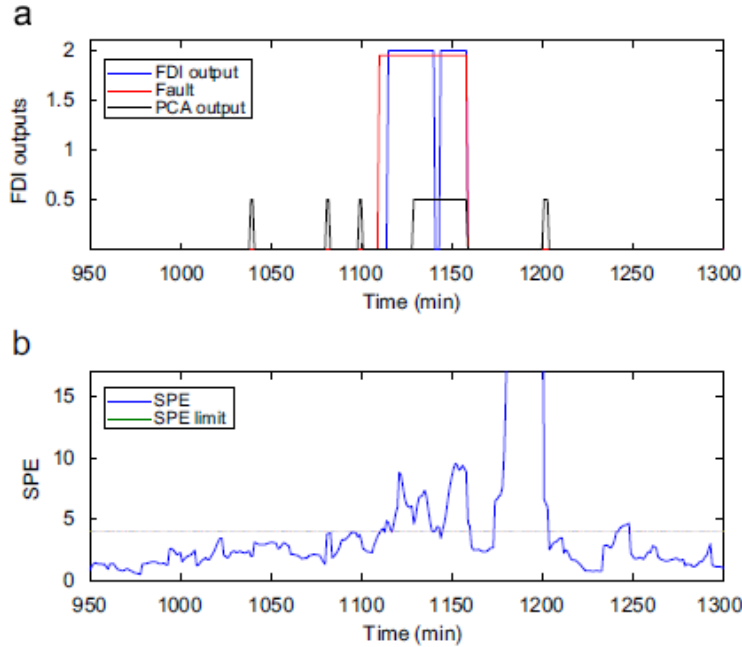


**Fig. 6.** (a) Monitoring results for the effluent analyzer measurement error case  
(b) SPE index over time range for the effluent analyzer measurement error case

A contribution plot during the fault in the effluent analyzer at time 1149 is shown in Fig. 7. As can be seen from the graphs in Fig. 7, the effluent ethylene to feed ethane ratio (variable 9), sum of feed components to sum of effluent components ratio (variable 14), effluent ethylene to HC feed (variable 22) and effluent ethylene content (variable 3) had the largest effect on the high SPE value. All of them included the effluent ethylene content in the variable.

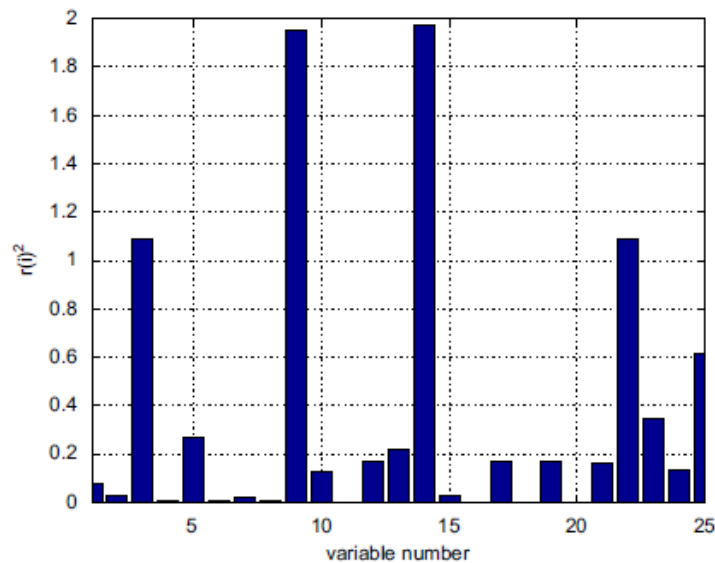


**Fig. 7.** A contribution plot during the fault in the effluent analyzer at time 1149

The actual measurement of the ethylene content (blue line) and its estimation produced by PCA (red line) are compared in Fig. 8. As can be seen, the actual measurement of the fault state is 0.7 mol% higher than the estimation. The stored chromatograph records indicate that the effluent analyzer had in fact produced too high values for the ethylene content at this time.

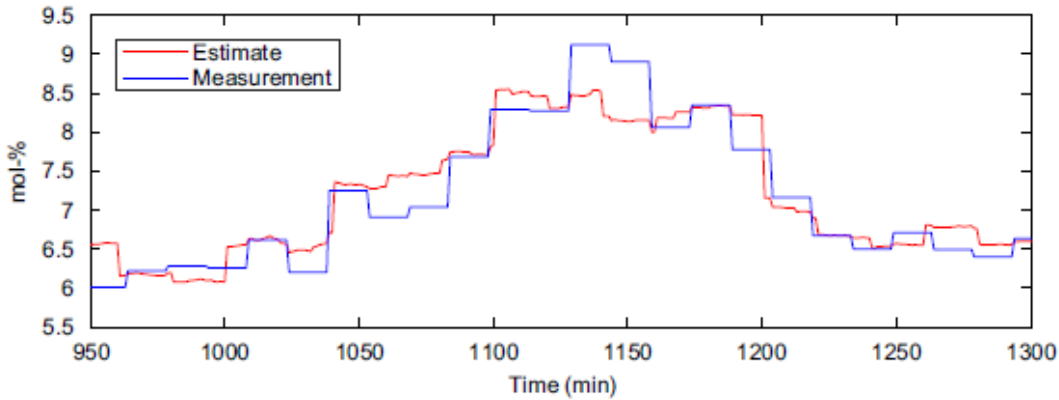


**Fig. 8.** Effluent ethane content measurement (blue) and its estimate (red)

#### 5.1.2. Case 2: error in feed analyzer measurement

The performance of the FDI system during a measurement error of the feed analyzer is discussed next. In the case of an error in the feed analyzer, the analysis results of the diagnosis system for the corresponding portion of the test data are shown in Fig. 9a, and the SPE index and in Fig. 9b.

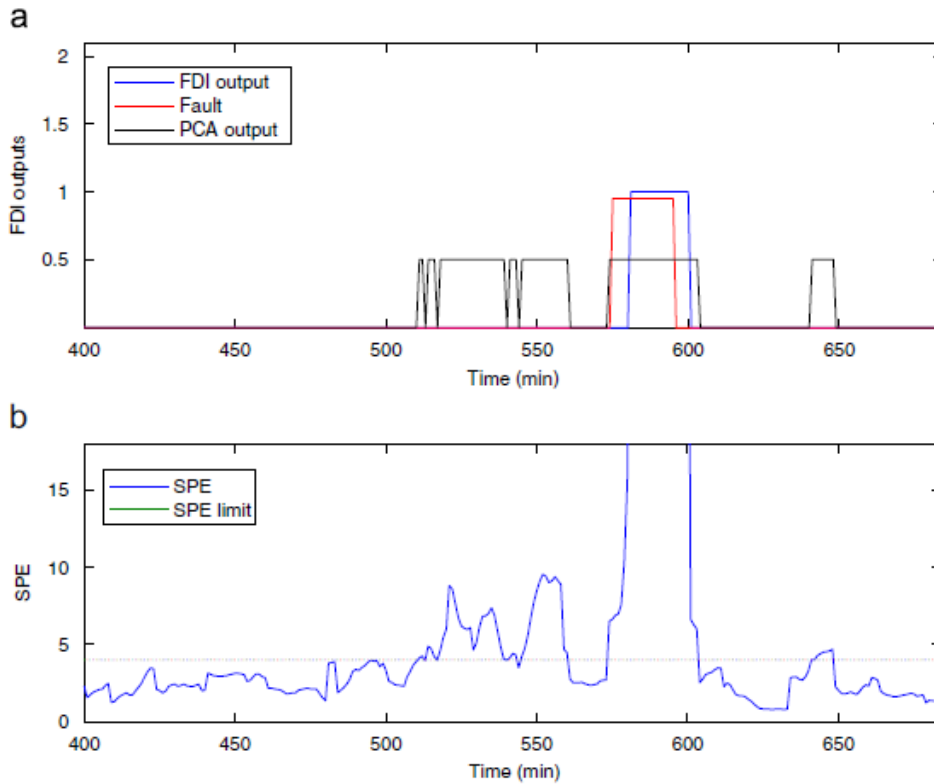


**Fig. 9.** (a) Monitoring results for the feed analyzer measurement error case  
(b) SPE index over time range for the feed analyzer measurement error case

The analyzer diagnosis system detected disturbances, some of which were classified as feed analyzer faults. The first alerts from SPE threshold crossings were generated as a result of large variations in the coil temperatures. However, at time 580 the SPE index rises sharply above the maximum value of the Y-axis, and falls back to normal at around time 600. It is a clear indication of an error in the feed analyzer and it was clearly identified also by the NNs. Trends in the hydrocarbon composition of the feed are shown in Fig. 10. The identified erroneous analyzer measurement differs noticeably from the other measurements during the period.

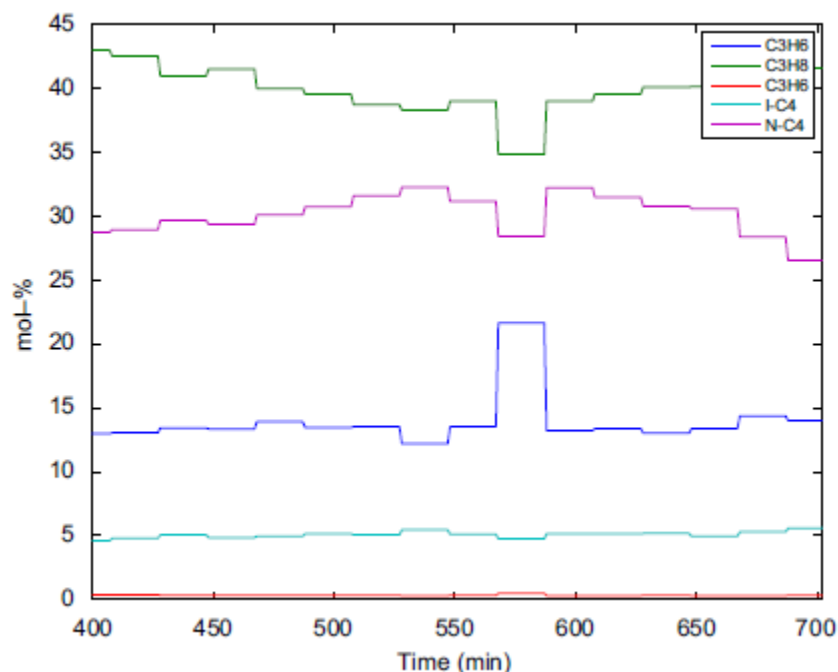


**Fig. 10.** Feedstock component contents over a 5 h period

### 5.1.3. Case 3: the performance of the FDI system under process disturbances

The performance of the system under faulty conditions for faults other than analyzer faults is now illustrated. A case where variations in the fuel gas causes process disturbance is examined in more detail. The analysis results of the diagnosis system on a portion of the test data are shown in Fig. 11a. The SPE index for the same time period is also presented in Fig. 11b. The SPE index continuously crossed the threshold value and generated alerts. The system detected a fault from the SPE values, but the NNs did not diagnose it as a fault of either of the analyzers.

The fluctuation in the coil outlet temperature is shown in Fig. 12. The outlet temperature starts to swing during the time range as a result of fluctuations in the fuel gas. This is a disturbance that influences the coil outlet temperatures and effluent contents of the furnace. Because of the added robustness provided by two different kinds of NN, the FDI system was able to correctly diagnose the situation as a non-analyzer fault.



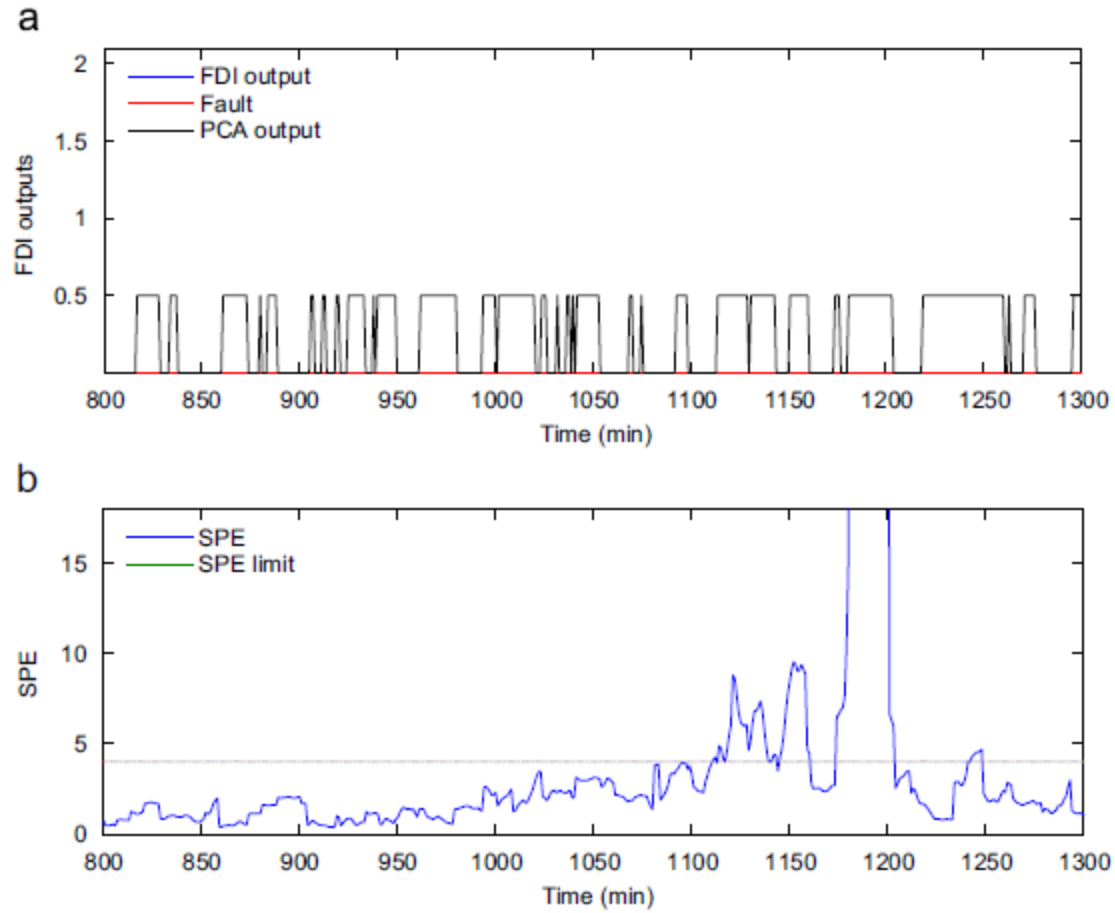


**Fig. 11.** (a) Monitoring results during disturbance caused by variations in the fuel gas  
(b) SPE index over time range during disturbance caused by variations in the fuel gas

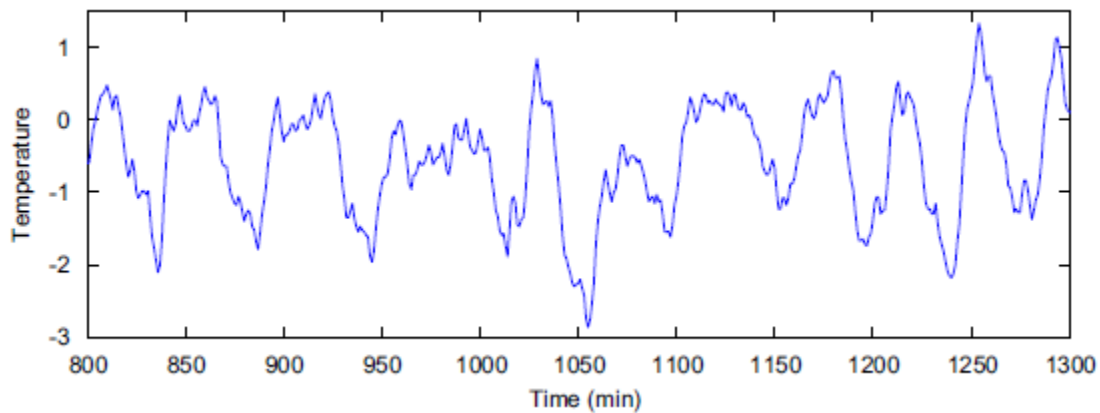


**Fig. 12.** Fluctuation in the coil outlet temperature

### 5.2 Comparative analysis of a combination of PCA and NNs

A comparative study was performed to determine the effect of combining PCA and NNs into a single method. The main reason for combining the PCA and NNs into a single system was that the methods alone were unable to provide sufficiently reliable fault detection and isolation. In this industrial case, the

reliability of the fault isolation was the most important criterion for the FDI system. It was especially important to avoid false alarms, even at the cost of introducing some classification delay or some missed detections.

The results of the study are summarized in Table 2. As is shown in the table the proposed system, the combination of SOM and RBFN, and the combination of PCA, SOM and RBFN produced the lowest number of false alarms. Thus, by combining several methods, it is possible to reduce the number of false alarms generated by the system.

**Table 2**

A comparative study of the FDI systems

Combination	Correct classification To normal state	False alarms	Correct classification of faults
SOM+RBFN+PCA	99.8	0.2	60
SOM+RBFN	99.8	0.2	80
SOM+PCA	96.6	3.4	61.4
RBFN+PCA	99.4	0.6	64.3
SOM	84.3	15.6	81.4
RBFN	97.9	2.1	91.4

Special attention was paid in constructing the inputs, particularly the computed variables in the set up of the FDI system. Although the use of computed variables has been a common practice among chemical engineers in industry for decades, their use is not yet well established in FDI nor in control applications.

To study the effect of computed variables in this application, a comparative study was carried out in which the performance of the FDI system with and without computed variables was compared. The FDI system was set up in the first case using only direct measurements as inputs, and in the second with the computed variables. Since the dimension of the input set without computed variables was considerably smaller, the dimensions of the FDI systems were modified. The PCA model without computed variables included five latent variables that captured 95% of the variation, but for the NNs smaller network sizes were used. The performance of the systems with and without computed variables was tested with the same data set. As shown in Table 3, for all cases the systems with computed variables performed considerably better and produced fewer false alarms and higher correct classification percentages. Therefore, the utilization of computed variables was justified in this application.

**Table 3**

Performance of the FDI system with and without computed variables

Combination	Input set	Correct classification to normal state	False alarms	Correct classification of faults
SOM+RBFN+PCA	With c.v.	99.8	0.2	60
	Without c.v.	99.5	0.5	0
SOM+RBFN	With c.v.	99.8	0.2	80
	Without c.v.	96.5	3.6	12.9
SOM+PCA	With c.v.	96.6	3.4	61.4
	Without c.v.	99.5	0.5	0
RBFN+PCA	With c.v.	99.4	0.6	64.3
	Without c.v.	99.2	0.8	8.6
SOM	With c.v.	84.3	15.7	81.4
	Without c.v.	84.2	15.8	12.9
RBFN	With c.v.	97.9	2.1	91.4
	Without c.v.	54.6	45.4	78.6

## 6 Conclusions

This paper presents a fault detection and isolation system consisting of a combination of PCA and two neural networks (NNs), RBFN and SOM. The application of the proposed system gave promising results in identifying faulty operations of the on-line analyzers of the ethylene cracking process.

The final on-line analyzer diagnosis system was able to detect and isolate faults from the process data without long delays. The system was also able to detect process disturbances caused by reasons other than analyzer faults

Process knowledge had an important role in the selection of variables for the PCA and NNs models. The “process-wise” variables, computed on the basis of the raw measurements, significantly improved the detection and isolation of process faults. The redundancy resulting from combining the principal component analysis and two NNs gave more reliable results than using only one diagnosis method. This was especially the case with process data, when principal component analysis detected unknown process disturbances. This study indicates that a system employing only one method may not be able to meet all the requirements for an industrial diagnosis system. Integrating complementary methods to perform collective problem solving is a recommended concept for future improvements in diagnostic systems.

## Acknowledgments

The authors acknowledge the encouragement and stimulating discussions with the personnel of Neste Jacobs Oy and the support of Borealis Polymers Oy. This research was supported by the National Technology Agency of Finland, which is gratefully acknowledged.

## References

- Bakshi, B. R., & Stephanopoulos, G. (1993). Wavenet: A multiresolution hierarchical neural network with localised learning. *A.I.Ch.E. Journal*, 39(1), 57–81.
- Bergman, S., Sourander, M., & Jämsä-Jounela, S.-L. (2002). Monitoring of an industrial dearomatisation process. In: *Proceedings of the 15<sup>th</sup> IFAC world congress on automatic control*, Barcelona, Spain, July 2002.
- Broomhead, D. S., & Lowe, D. (1988). Multivariable functional interpolation and adaptive networks. *Complex Systems*, 2(3), 312–355.
- Chen, G., McAvoy, T. J., & Piovoso, M. J. (1998). A multivariate statistical controller for online quality improvement. *Journal of Process Control*, 8, 139–149.
- Chiang, L. H., Russell, E. L., & Braatz, R. D. (2000). Fault diagnosis in chemical processes using Fisher discriminant analysis, discriminant partial least squares, and principal component analysis. *Chemometrics and Intelligent Laboratory Systems*, 50(2), 243–252.
- Dong, D., & McAvoy, T. J. (1996). Nonlinear principal component analysis—Based on principal curves and neural networks. *Computers and Chemical Engineering*, 20, 65–78.
- Gnanadesikan, R. (1977). *Methods for statistical data analysis of multivariate observations* (1st ed.). New York: Wiley.
- Isermann, R., & Ballé, P. (1997). Trends in the application of model-based fault detection and diagnosis of technical processes. *Control Engineering Practice*, 5(5), 709–719.
- Jämsä-Jounela, S.-L., Laine, S., & Ruokonen, E. (1998). Ore type based expert systems in mineral processing plants. *Particle and Particle Systems Characterization*, 15, 200–207.
- Jämsä-Jounela, S.-L., Vermasvuori, M., Enden, P., & Haavisto, S. (2003). A process monitoring system based on the Kohonen self-organizing maps. *Control Engineering Practice*, 11, 83–92.
- Jolliffe, I. T. (2002). *Principal component analysis* (2nd ed.). New York: Springer.

- Kämpjärvi, P., (2002). M.Sc. thesis, Helsinki University of Technology, Department of Chemical Technology, (p. 106).
- Kohonen, T. (1990). The Self-organizing Map. *Proceedings of the IEEE*, 78, 1464–1480.
- Komulainen, T., Sourander, M., & Jaämsä-Jounela, S.-L. (2004). An online application of dynamic PLS to dearomatization process. *Computers and Chemical Engineering*, 28, 2611–2619.
- Ku, W., Storer, R. H., & Georgakis, C. (1995). Disturbance detection and isolation by dynamic principal component analysis. *Chemometrics and Intelligent Laboratory Systems*, 30, 179–196.
- Li, W., Yue, H. H., Valle-Cervantes, S., & Qin, S. J. (2000). Recursive PCA for adaptive process monitoring. *Journal of Process Control*, 10, 471–486.
- Misra, M., Yue, H. H., Qin, S. J., & Ling, C. (2002). Multivariate process monitoring and fault diagnosis by multi-scale PCA. *Computers and Chemical Engineering*, 26, 1281–1293.
- Moody, J., & Darken, C. J. (1989). Fast learning in networks of locally tuned processing units. *Neural Computation*, 1, 151–160.
- Patton, R.J., Uppal, F.J., & Lopez-Toribio, C.J. (2000). Soft computing approaches to fault diagnosis for dynamic systems: a survey. In: *Proceedings of IFAC symposium on fault detection, supervision and safety for technical processes*, Budapest, Hungary, (pp. 298–311).
- Pranatyasto, T. N., & Qin, S. J. (2001). Sensor validation and process fault diagnosis for FCC units under MPC feedback. *Control Engineering Practice*, 9, 877–888.
- Qin, S. J. (1998). Recursive PLS algorithms for adaptive data modeling. *Computers and Chemical Engineering*, 22(4), 503–514.
- Rallo, R., Ferre-Gine, J., Arenas, A., & Giralt, F. (2002). Neural virtual sensor for the inferential prediction of product quality from process variables. *Computers and Chemical Engineering*, 26(12), 1735–1754.
- Venkatasubramanian, V., Rengaswamy, R., Kavuri, S. N., & Yin, K. (2003). A review of process fault detection and diagnosis Part III: Process history based methods. *Computers and Chemical Engineering*, 27(3), 327–346.
- Venkatasubramanian, V., Rengaswamy, R., Yin, K., & Kavuri, S. N. (2003). A review of process fault detection and diagnosis Part I: Quantitative model-based methods. *Computers and Chemical Engineering*, 27(3), 293–311.
- Wienke, D., van den Broek, W., Buydens, L., Huth-Fehre, T., Feldhoff, R., Kantimm, T., et al. (1996). Adaptive resonance theory based neural network for supervised chemical pattern recognition (FuzzyARTMAP) Part 2: Classification of post-consumer plastics by remote NIR spectroscopy using an InGaAs diode array. *Chemometrics and Intelligent Laboratory Systems*, 32(2), 165–176.
- Yoon, S., & MacGregor, J.F. (2001). Incorporation of external information into multivariate PCA/PLS models. In: Stephanopoulos, G., Romagnoli, J.A., & Yoon, E.S., (Eds.), *Proceedings of the fourth IFAC workshop on on-line fault detection and supervision in the chemical process industries*, Korea (pp. 384).
- Zhao, J., Chen, B., & Shen, J. (1998). Multidimensional non-orthogonal wavelet-sigmoid basis function neural network for dynamic process fault diagnosis. *Computers and Chemical Engineering*, 23, 83–92.